

Fully Automatic Self-Calibrated Conductivity Measurement System

By **Robert Lee** and **Walt Kester**

Share on   

Introduction

The increasing importance of monitoring water quality has led to the development of a number of related sensors and signal conditioning circuits. Water quality is measured in terms of bacteria count, pH level, chemical content, turbidity, and conductivity. All aqueous solutions conduct electricity to some degree. Adding electrolytes such as salts, acids, or bases to pure water increases the conductivity and decreases resistivity. This article focuses on conductivity measurements.

Pure water does not contain significant amounts of electrolytes and conducts only a small amount of electric current when a sample is subjected to an applied voltage—its conductivity is therefore low. On the other hand, a large quantity of electrolytes in the sample causes more current to be conducted—its conductivity is higher.

It is more common to think in terms of resistance rather than conductance, but the two are reciprocals. The resistivity, ρ , of a material or liquid is defined as the resistance of a cube of the material with perfectly conductive contacts on opposite faces. The resistance, R , for other shapes, can be calculated by

$$R = \rho L/A \quad (1)$$

where:

L is the distance between the contacts.

A is the area of the contacts.

Resistivity is measured in units of $\Omega \text{ cm}$. A $1 \Omega \text{ cm}$ material has a resistance of 1Ω when contacted on opposite faces of a $1 \text{ cm} \times 1 \text{ cm} \times 1 \text{ cm}$ cube.

Conductance is simply the reciprocal of resistance, and conductivity is the reciprocal of resistivity. The unit of measurement of conductance is siemens (S), and the unit of measurement of conductivity is S/cm, mS/cm, or $\mu\text{S/cm}$.

For the purposes of this article, Y is the general symbol for conductivity measured in S/cm, mS/cm, or $\mu\text{S/cm}$. However, in many cases, the distance term is dropped for convenience, and the conductivity is simply expressed as S, mS, or μS .

Measuring Conductivity Using Conductivity Cells

A conductivity system measures conductivity by means of electronics connected to a sensor, called a conductivity cell, immersed in a solution, as shown in Figure 1.

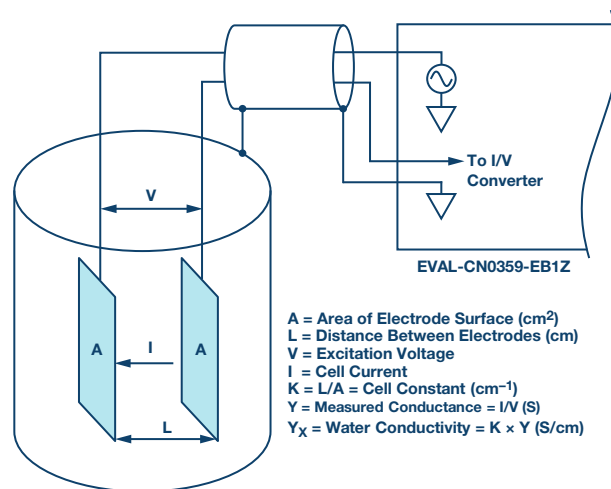


Figure 1. Interface between conductivity cell and electronics (EVAL-CN0359-EB1Z).

The electronic circuitry impresses an alternating voltage on the sensor and measures the size of the resulting current, which is related to the conductivity. Because conductivity has a large temperature coefficient (up to $4\%/^{\circ}\text{C}$), an integral temperature sensor is incorporated into the circuitry to adjust the reading to a standard temperature, usually 25°C (77°F). When measuring solutions, the temperature coefficient of the conductivity of the water itself must be considered. To compensate accurately for the temperature, a second temperature sensor and compensation network must be used.

The contacting type sensor typically consists of two electrodes that are insulated from one another. The electrodes, typically Type 316 stainless steel, titanium palladium alloy, or graphite, are specifically sized and spaced to provide a known cell constant. Theoretically, a cell constant of $1.0/\text{cm}$ describes two electrodes, each sized 1 cm^2 in area, and spaced 1 cm apart. Cell constants must be matched to the measurement system for a given range of operation. For instance, if a sensor with a cell constant of $1.0/\text{cm}$ is used in pure water with a conductivity of $1 \mu\text{S/cm}$, the cell has a resistance of $1 \text{ M}\Omega$. Conversely, the same cell in seawater has a resistance of 30Ω . Because the resistance ratio is so large, it is difficult for ordinary instruments to accurately measure such extremes with only one cell constant.

When measuring the 1 $\mu\text{S}/\text{cm}$ solution, the cell is configured with large area electrodes spaced a small distance apart. For example, a cell with a cell constant of 0.01/cm results in a measured cell resistance of approximately 10 k Ω rather than 1 M Ω . It is easier to accurately measure 10 k Ω than 1 M Ω ; therefore, the measuring instrument can operate over the same range of cell resistance for both ultrapure water and high conductivity seawater by using cells with different cell constants.

The cell constant, K , is defined as the ratio of the distance between the electrodes, L , to the area of the electrodes, A :

$$K = L/A \quad (2)$$

The instrumentation then measures the cell conductance, Y :

$$Y = I/V \quad (3)$$

The conductivity of the liquid, Y_x , is then calculated:

$$YX = K \times Y \quad (4)$$

There are two types of conductivity cells: those with two electrodes and those with four electrodes, as shown in Figure 2. The electrodes are often referred to as poles.

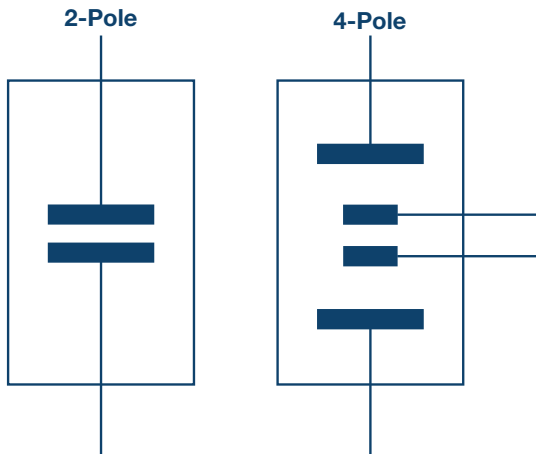


Figure 2. 2-pole and 4-pole conductivity cells.

The 2-pole sensor is more suitable for low conductivity measurements, such as purified water, and various biological and pharmaceutical liquids. The 4-pole sensor is more suitable for high conductivity measurements, such as waste water and seawater analysis.

The cell constants for 2-pole cells range from approximately 0.1/cm to 1/cm, and the cell constants for 4-pole cells range from 1/cm to 10/cm.

The 4-pole cell eliminates the errors introduced by polarization of the electrodes and field effects that can interfere with the measurement.

The actual configuration of the electrodes can be that of parallel rings, coaxial conductors, or others, rather than the simple parallel plates shown in Figure 2.

Regardless of the type of cell, it is important not to apply a dc voltage to any electrode because ions in the liquid will accumulate on the electrode surface, thereby causing polarization, measurement errors, and damage to the electrode.

Take special care with sensors that have shields, as in the case of coaxial sensors. The shield must be connected to the same potential as the metal container holding the liquid. If the container is grounded, the shield must be connected to the circuit board ground.

The final precaution is not to exceed the rated excitation voltage or current for the cell. The following circuit allows programmable excitation voltages from 100 mV to 10 V, and the R23 (1 k Ω) series resistor limits the maximum cell current to 10 mA.

Circuit Description

The circuit shown in Figure 3 is a completely self-contained, microprocessor controlled, highly accurate conductivity measurement system that is ideal for measuring the ionic content of liquids, water quality analysis, industrial quality control, and chemical analysis.

A carefully selected combination of precision signal conditioning components yields an accuracy of better than 0.3% over a conductivity range of 0.1 μS to 10 S (10 M Ω to 0.1 Ω) with no calibration requirements.

Automatic detection is provided for either 100 Ω or 1000 Ω platinum (Pt) resistance temperature devices (RTDs), allowing the conductivity measurement to be referenced to room temperature.

The system accommodates 2- or 4-wire conductivity cells, and 2-, 3-, or 4-wire RTDs for added accuracy and flexibility.

The circuit generates a precise ac excitation voltage with minimum dc offset to avoid a damaging polarization voltage on the conductivity electrodes. The amplitude and frequency of the ac excitation is user-programmable.

An innovative synchronous sampling technique converts the peak-to-peak amplitude of the excitation voltage and current to a dc value for accuracy and ease in processing using the dual, 24-bit Σ - Δ ADC contained within the precision analog microcontroller.

The intuitive user interface is an LCD display and an encoder push button. The circuit can communicate with a PC using an RS-485 interface if desired, and it operates on a single 4 V to 7 V supply.

The excitation square wave for the conductivity cell is generated by switching the ADG1419 between the +VEXC and -VEXC voltages using the PWM output of the ADuCM360 microcontroller. It is important that the square wave has a precise 50% duty cycle and a very low dc offset. Even small dc offsets can damage the cell over a period of time.

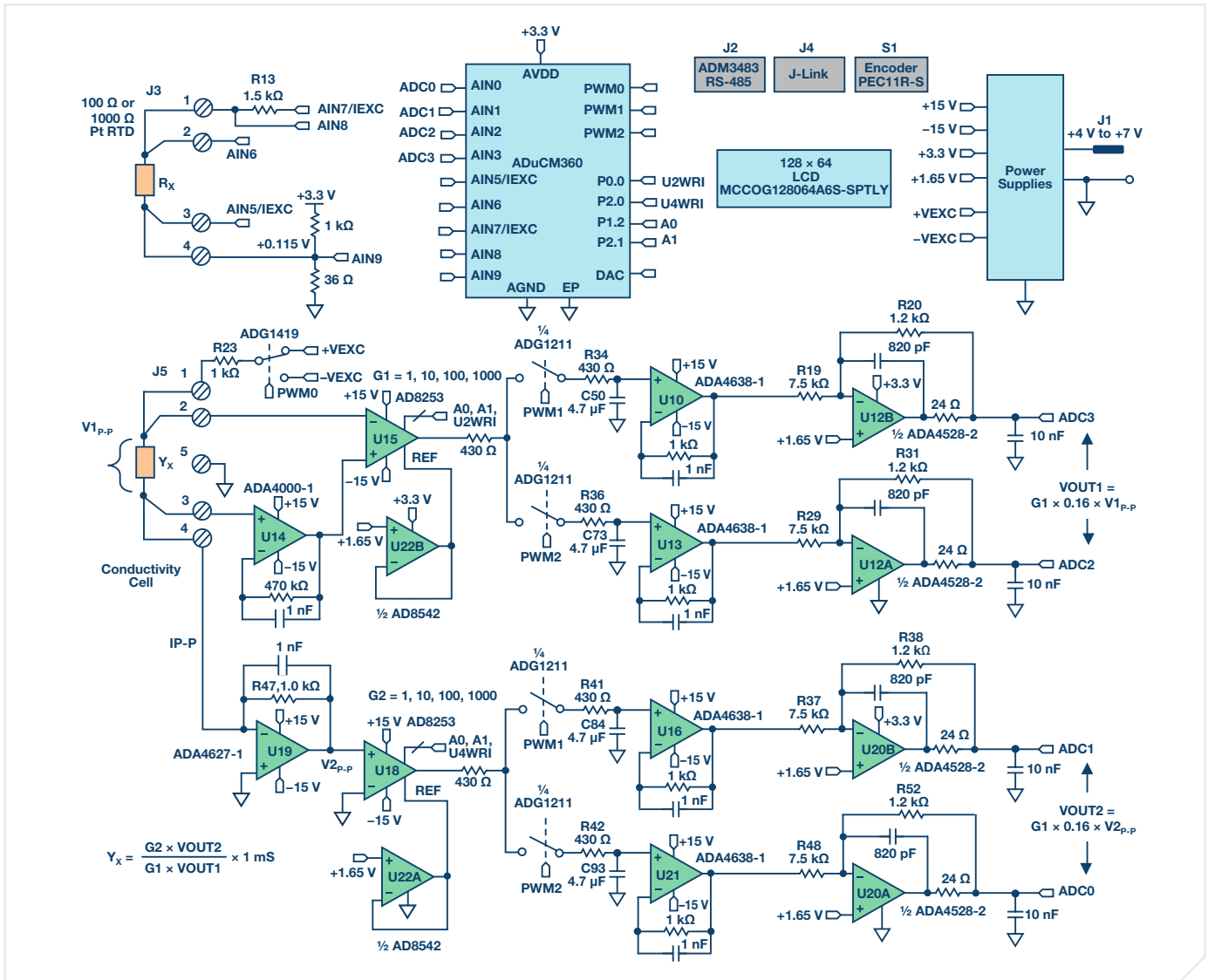


Figure 3. High performance conductivity measurement system (simplified schematic: all connections and decoupling not shown).

The +VEXC and -VEXC voltages are generated by the ADA4077-2 op amps (U9A and U9B), and their amplitudes are controlled by the DAC output of the ADuCM360, as shown in Figure 4.

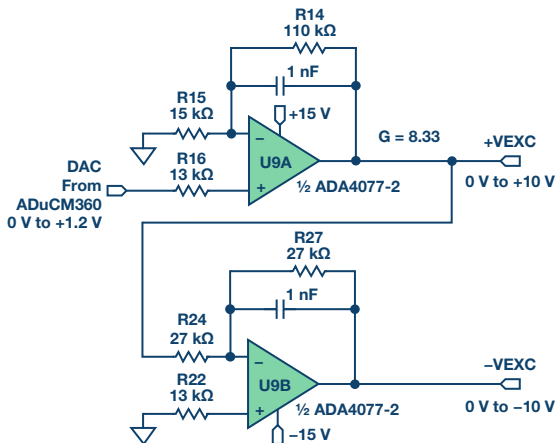


Figure 4. Excitation voltage sources.

The ADA4077-2 has a typical offset voltage of 15 μ V (A grade), a 0.4 nA bias current, a 0.1 nA offset current, and an output current of up to \pm 10 mA, with

a dropout voltage of less than 1.2 V. The U9A op amp has a closed-loop gain of 8.33 and converts the ADuCM360 internal DAC output (0 V to 1.2 V) to the +VEXC voltage of 0 V to 10 V. The U9B op amp inverts the +VEXC and generates the -VEXC voltage. R22 is chosen such that $R22 = R24 \parallel R27$ to achieve first-order bias current cancellation. The error due to the 15 μ V offset voltage of U9A is approximately $(2 \times 15 \mu\text{V}) \div 10 \text{ V} = 3 \text{ ppm}$. The primary error introduced by the inverting stage is therefore the error in the resistor matching between R24 and R27.

The ADG1419 is a 2.1 Ω , on-resistance SPDT analog switch with an on-resistance flatness of 50 m Ω over a \pm 10 V range, making it ideal for generating a symmetrical square wave from the \pm VEXC voltages. The symmetry error introduced by the ADG1419 is typically $50 \text{ m}\Omega \div 1 \text{ k}\Omega = 50 \text{ ppm}$. Resistor R23 limits the maximum current through the sensor to $10 \text{ V} / 1 \text{ k}\Omega = 10 \text{ mA}$.

The voltage applied to the cell, V1, is measured with the AD8253 instrumentation amplifier (U15). The positive input to U15 is buffered by the ADA4000-1 (U14). The ADA4000-1 is chosen because of its low bias current of 5 pA to minimize the error in measuring low currents associated with low conductivities. The negative input of the AD8253 does not require buffering.

The offset voltages of U14 and U15 are removed by the synchronous sampling stage and do not affect the measurement accuracy.

U15 and U18 are AD8253 10 MHz, 20 V/μs, programmable gain (G = 1, 10, 100, 1000) instrumentation amplifiers with gain error of less than 0.04%. The AD8253 has a slew rate of 20 V/μs and a settling time of 1.8 μs to 0.001% for G = 1000. Its common-mode rejection is typically 120 dB.

The U19 (ADA4627-1) stage is a precision current to voltage converter that converts the current through the sensor to voltage. The ADA4627-1 has an offset voltage of 120 μV (typical, A grade), a bias current of 1 pA (typical), a slew rate of 40 V/μs, and a 550 ns settling time to 0.01%. The low bias current and offset voltage make it ideal for this stage. The symmetry error produced by the 120 μV offset error is only 120 μV/10 V = 12 ppm.

The U22A and U22B (AD8542) buffers supply the 1.65 V reference to the U18 and U15 instrumentation amplifiers, respectively.

The following is a description of the remainder of the signal path in the voltage channel (U17A, U17B, U10, U13, U12A, and U12B). The operation of the current channel (U17C, U17D, U16, U21, U20A, and U20B) is identical.

The ADuCM360 generates the PWM0 square wave switching signal for the ADG1419 switch as well as PWM1 and PWM2 synchronizing signals for the synchronous sampling stages. The cell voltage and the three timing waveforms are shown in Figure 5.

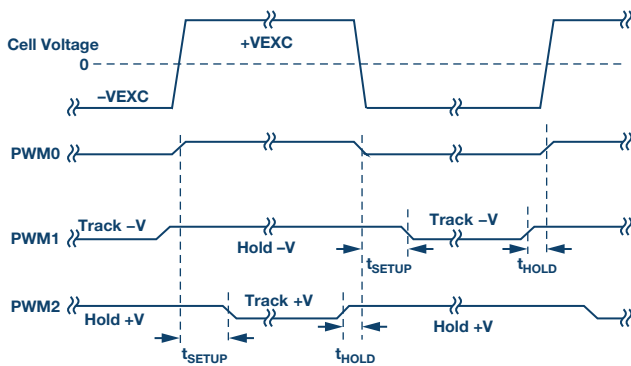


Figure 5. Cell voltage and track-and-hold timing signals.

The output of the AD8253 in amp (U15) drives two parallel track-and-hold circuits composed of ADG1211 switches (U17A/U17B), series resistors (R34/R36), hold capacitors (C50/C73), and unity-gain buffers (U10/U13).

The ADG1211 is a low charge injection, quad SPST analog switch, operating on a ±15 V power supply with up to ±10 V input signals. The maximum charge injection due to switching is 4 pC, which produces a voltage error of only 4 pC ÷ 4.7 μF = 0.9 μV.

The PWM1 signal causes the U10 track-and-hold buffer to track the negative cycle of the sensor voltage and then hold it until the next track cycle. The output of the U10 track-and-hold buffer is therefore a dc level corresponding to the negative amplitude of the sensor voltage square wave.

Similarly, the PWM2 signal causes the U13 track-and-hold buffer to track the positive cycle of the sensor voltage and then hold it until the next track cycle. The output of the U13 track-and-hold buffer is therefore a dc level corresponding to the positive amplitude of the sensor voltage square wave.

The bias current of the track-and-hold buffers (ADA4638-1) is 45 pA typical, and the leakage current of the ADG1211 switch is 20 pA typical. Therefore, the worst-case leakage current on the 4.7 μF hold capacitors is 65 pA. For a 100 Hz excitation frequency, the period is 10 ms. The drop voltage over one-half the period (5 ms) due to the 65 pA leakage current is (65 pA × 5 ms) ÷ 4.7 μF = 0.07 μV.

The offset voltage of the ADA4638-1 zero-drift amplifier is only 0.5 μV typical and contributes negligible error.

The final stages in the signal chain before the ADC are the ADA4528-2 inverting attenuators (U12A and U12B) that have a gain of -0.16 and a common-mode output voltage of +1.65 V. The ADA4528-2 has an offset voltage of 0.3 μV typical and therefore contributes negligible error.

The attenuator stage reduces the ±10 V maximum signal to ±1.6 V with a common-mode voltage of 1.65 V. This range is compatible with the input range of the ADuCM360 ADC input, which is 0 V to 3.3 V (1.65 V ± 1.65 V) for an AVDD supply of 3.3 V.

The attenuator stages also provide noise filtering and have a -3 dB frequency of approximately 198 kHz.

The differential output of the voltage channel, VOUT1, is applied to the AIN2 and AIN3 inputs of the ADuCM360. The differential output of the current channel, VOUT2, is applied to the AIN0 and AIN1 inputs of the ADuCM360.

The equations for the two outputs are given by

$$VOUT1 = G1 \times 0.16 \times V1_{p,p} \quad (5)$$

$$VOUT2 = G2 \times 0.16 \times V2_{p,p} \quad (6)$$

The cell current is given by

$$I_{p,p} = V1_{p,p} \times YX \quad (7)$$

The V2_{p,p} voltage is given by

$$V2_{p,p} = I_{p,p} \times R47 \quad (8)$$

Solving Equation 8 for I_{p,p} and substituting into Equation 7 yields the following for Y_X:

$$YX = \frac{V2_{p,p}}{V1_{p,p} \times R47} \quad (9)$$

Solving Equation 5 and Equation 6 for V1_{p,p} and V2_{p,p} and substituting into Equation 9 yields the following:

$$YX = \frac{G2 \times VOUT2}{G1 \times VOUT1 \times R47} \quad (10)$$

$$YX = \frac{G2 \times VOUT2}{G1 \times VOUT1} \times 1 \text{ mS} \quad (11)$$

Equation 11 shows that the conductivity measurement depends on G1, G2, and R47, and the ratio of VOUT2 to VOUT1. Therefore, a precision reference is not required for the ADCs within the ADuCM360.

The AD8253 gain error (G1 and G2) is 0.04% maximum, and R47 is chosen to be a 0.1% tolerance resistor.

From this point, the resistors in the VOUT1 and VOUT2 signal chain determine the overall system accuracy.

The software sets the gain of each AD8253 as follows:

- ▶ If the ADC code is over 94% of full scale, the gain of the AD8253 is reduced by a factor of 10 on the next sample.
- ▶ If the ADC code is less than 8.8% of full scale, the gain of the AD8253 is increased by a factor of 10 on the next sample.

The 3-wire connection is another popular RTD configuration that eliminates lead resistance errors, as shown in Figure 8.

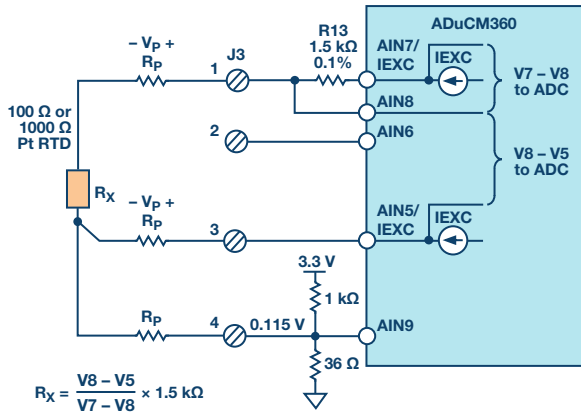


Figure 8. Configuration for 3-wire RTD connection.

The second matched IEXC current source (AIN5/IEXC) develops a voltage across the lead resistance in series with Terminal 3 that cancels the voltage dropped across the lead resistance in series with Terminal 1. The measured $V8 - V5$ voltage is therefore free of lead resistance error.

Figure 9 shows the 2-wire RTD configuration where there is no compensation for lead resistance.

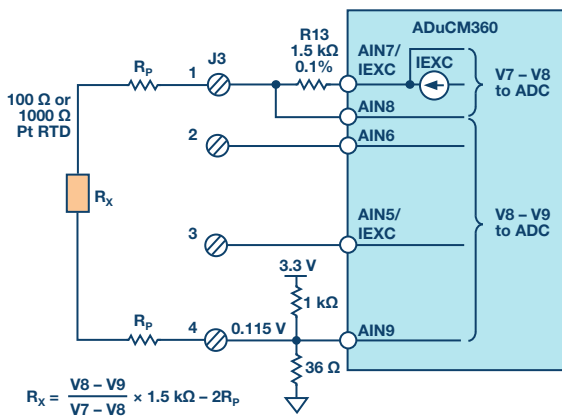


Figure 9. Configuration for 2-wire RTD connection.

The 2-wire configuration is the lowest cost circuit and is suitable for less critical applications, short RTD connections, and higher resistance RTDs such as Pt1000.

Power Supply Circuits

To simplify system requirements, all the required voltages ($\pm 15 \text{ V}$ and $+3.3 \text{ V}$) are generated from a single 4 V to 7 V supply, as shown in Figure 10.

The ADP2300 buck regulator generates the 3.3 V supply for the board. The design is based on the downloadable [ADP230x Buck Regulator Design Tool](#).

The ADP1613 boost regulator generates a regulated $+15 \text{ V}$ supply and an unregulated -15 V supply. The -15 V supply is generated with a charge pump. The design is based on the [ADP161x Boost Regulator Design Tool](#).

Details regarding the selection and design of power supplies are available at www.analog.com/ADIsimPower.

Use proper layout and grounding techniques to prevent the switching regulator noise from coupling into the analog circuits. See the [Linear Circuit Design Handbook](#), the [Data Conversion Handbook](#), the [MT-031 Tutorial](#), and the [MT-101 Tutorial](#) for further details.

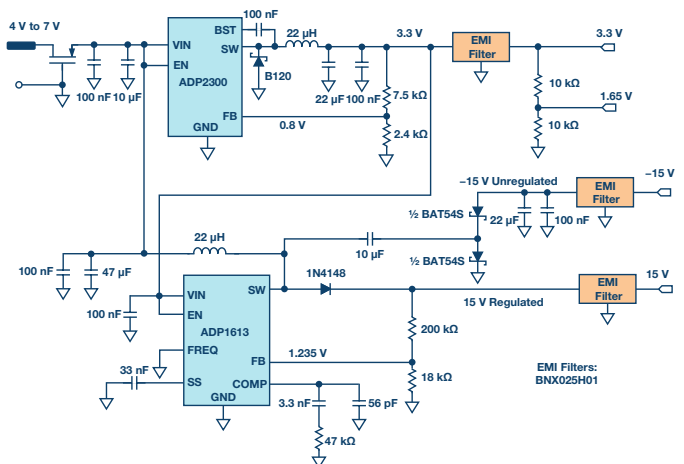


Figure 10. Power supply circuits.

Figure 11 shows the LCD backlight driver circuit.

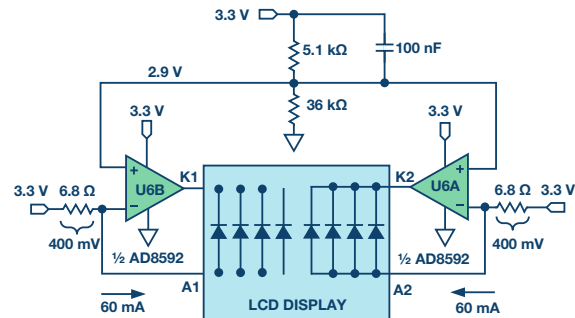


Figure 11. LCD backlight drivers.

Each half of the AD8592 op amp acts as a 60 mA current source to supply the LCD backlight currents. The AD8592 can source and sink up to 250 mA , and the 100 nF capacitor ensures a soft startup.

Hardware, Software, and User Interface

The complete circuit including software is available as the [CN-0359 Circuits from the Lab Reference Design](#). The circuit board, [EVAL-CN0359-EB1Z](#), comes preloaded with the code required to make the conductivity measurements. The actual code can be found in the CN-0359 Design Support Package, in the [CN0359-SourceCode.zip](#) file.

The user interface is intuitive and easy to use. All user inputs are from a dual function push button/rotary encoder knob. The encoder knob can be turned clockwise or counterclockwise (no mechanical stop), and can also be used as a push button.

Figure 12 is a photo of the EVAL-CN0359-EB1Z board that shows the LCD display and the position of the encoder knob.



Figure 12. Photo of an EVAL-CN0359-EB1Z board showing the home screen in measurement mode.

After connecting, the conductivity cell and the RTD the board is powered up. The LCD screen appears as shown in Figure 12.

The encoder knob is used to input the excitation voltage, excitation frequency, temperature coefficient of the conductivity cell, the cell constant, setup time, hold time, RS-485 baud rate and address, LCD contrast, and so forth. Figure 13 shows some of the LCD display screens.

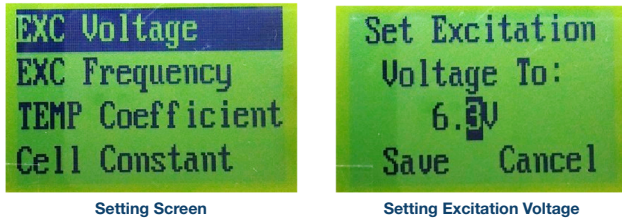


Figure 13. LCD display screens.

The EVAL-CN0359-EB1Z is designed to be powered with the EVAL-CFTL-6V-PWRZ 6 V power supply. The EVAL-CN0359-EB1Z requires only the power supply and the external conductivity cell and RTD for operation.

The EVAL-CN0359-EB1Z also has an RS-485 connector, J2, that allows an external PC to interface with the board. Connector J4 is a JTAG/SWD interface for programming and debugging the ADuCM360.

Figure 14 is a typical PC connection diagram showing an RS-485 to USB adapter.

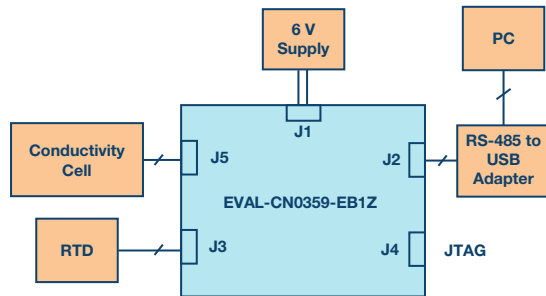


Figure 14. Test setup functional diagram.

Summary

The circuit described in this article is based on the Analog Devices CN-0359 reference design. Complete documentation including circuit note, detailed schematic, bill of material, layout, Gerber files, and source code is available at <http://www.analog.com/CN0359-DesignSupport>.

References

A Designer's Guide to Instrumentation Amplifiers, 3rd Edition. Analog Devices, Inc.

ADIsimPower Design Tool. Analog Devices, Inc.

CN-0359 Circuit Note, *Fully Automatic High Performance Conductivity Measurement System*. Analog Devices, Inc.

CN-0359 Design Support Package: www.analog.com/CN0359-DesignSupport. Analog Devices, Inc.

Linear Circuit Design Handbook. Analog Devices, Inc./Elsevier.

MT-031 Tutorial. *Grounding Data Converters and Solving the Mystery of "AGND" and "DGND."* Analog Devices, Inc.

MT-101 Tutorial. *Decoupling Techniques*. Analog Devices, Inc.

Op Amp Applications Handbook. Analog Devices, Inc./Elsevier.

"Section 7: Temperature Sensors" in *Sensor Signal Conditioning*. Analog Devices, Inc.

The Data Conversion Handbook. Analog Devices, Inc./Elsevier.

Data Sheets

[AD8253 Data Sheet](#).

[ADA4638-1 Data Sheet](#).

[AD8542 Data Sheet](#).

[ADG1211 Data Sheet](#).

[AD8592 Data Sheet](#).

[ADG1419 Data Sheet](#).

[ADA4000-1 Data Sheet](#).

[ADM3075 Data Sheet](#).

[ADA4077-2 Data Sheet](#).

[ADP2300 Data Sheet](#).

[ADA4528-2 Data Sheet](#).

[ADP1613 Data Sheet](#).

[ADA4627-1 Data Sheet](#).

[ADuCM360 Data Sheet](#).

Robert Lee [robert.lee@analog.com] has been an applications engineer at Analog Devices since January 2013. Robert received his B.S.E.E. from University of Electronic Science and Technology of China (UESTC) in 2004 and M.S.E.E. from UESTC in 2009. He has more than 10 years of embedded system design experience.



Robert Lee

Also by this Author:

[Complete Gas Sensor Circuit Using Nondispersive Infrared \(NDIR\)](#)
Volume 50, Number 4

Walt Kester [walt.kester@analog.com] is a corporate staff applications engineer at Analog Devices. During his many years at ADI, he has designed, developed, and given applications support for high speed ADCs, DACs, SHAs, op amps, and analog multiplexers. An author of many papers and articles, he prepared and edited 11 major applications books for ADI's global technical seminar series; topics include op amps, data conversion, power management, sensor signal conditioning, mixed-signal circuits, and practical analog design techniques. His latest book, *The Data Conversion Handbook* (Newnes), is a nearly 1000-page comprehensive guide to data conversion. Walt has a B.S.E.E. from NC State University and an M.S.E.E. from Duke University.



Walt Kester

Also by this Author:

[Complete Gas Sensor Circuit Using Nondispersive Infrared \(NDIR\)](#)
Volume 50, Number 4